Macromolecular Research, Vol. 23, No. 4, pp 341-349 (2015)
DOI 10.1007/s13233-015-3053-x

www.springer.com/13233
pISSN 1598-5032 eISSN 2092-7673

Photopolymerization Kinetic Studies of UV-Curable Sulfur-Containing Difunctional Acrylate Monomers Using Photo-DSC

Jin-Seung Kim[1], Si-Tae Noh[2], Jeong-Ohk Kweon[2], and Bong-Sang Cho*[,2]

[1]R&D center, Miwon Specialty Chemical, Ansan, Gyeonggi 425-100, Korea
[2]Department of Fine Chemical Engineering, College of Engineering Science, Hanyang University, Ansan, Gyeonggi 426-791, Korea

Received October 1, 2014; Revised January 26, 2015; Accepted January 27, 2015

Abstract: We synthesized UV-curable difunctional sulfur-containing thioacrylate and thiourethane acrylate with high refractive indices. The monomer structures were confirmed by nuclear magnetic resonance (NMR) spectroscopy and Fourier transform infrared spectroscopy (FTIR). The photopolymerization kinetics of 3,3'-thiobis(1-(phenylthio)propane-3,2-diyl) diacrylate (SMDA) and 4,12-dioxo-6,10-bis(phenylthiomethyl)-3,13-dioxa-8-thia-5,11-diazapentadecane-1,15-diyl diacrylate (SMUA) were investigated by photo-differential scanning calorimetry (photo-DSC). The effects of various parameters such as the UV intensity, temperature, photoinitiator concentration, and the type of initiator were evaluated. In SMDA, as the temperature and light intensity increased, the peak maximum time tended to decrease. The conversion increased with increasing temperature up to 60 °C and light intensity up to 20 mW/cm^2. The highest polymerization conversion was achieved with a PI concentration of 2.5% (w/w) with BK-6 as the PI. In SMUA, the rate of photopolymerization reached to the maximum value at 60 °C and 20 mW/cm^2. For the PI concentration, the maximum conversion and polymerization rate constant were the highest with 2.5% (w/w). Also the highest conversion of polymerization was achieved using HP-8 as the PI. The activation energies of SMDA and SMUA were 3.95 and 36.01 kJ/mol, respectively.

Keywords: acrylate monomer, photopolymerization, kinetics, photo-DSC.

Introduction

As alternatives to traditional thermally cured and solvent-based resins, UV-curable systems are widely used in various industries, because they possess numerous advantages including short processing times at room temperature, energy saving, the release of little or no volatile organic solvent, and high efficiencies. Consequently, a photopolymerization reaction process is attractive for many applications, such as coatings, inks, adhesives, optoelectronics and stereolithography.[1-3] Typically, (meth) acrylate monomers and oligomers are used in photopolymerization. Acrylate-containing monomers and oligomers are preferred due to the high reactivity of the acrylate double bond in radical polymerization.[4-6] Recently, the demand for UV-curable raw materials with a high refractive index has rapidly increased for use in brightness enhancing films, antireflective coatings, optical fiber coatings, plastic lenses, and other precision materials.[7-9]

The general approach to increasing the refractive indices of monomers is to introduce substituents with a high molar refraction, low molar volume, and high density, according to the Lorentz-Lorenz equation.[10] Among the various substituents, the sulfur atom is a good candidate because of its high atomic refraction. Also, sulfur-containing monomers possess optical transparency, a high dielectric constant, and strong adhesion to substrates.[11,12] Recently, the sulfur-containing monomers with high refractive index have been studied for optical applications. Khudyakov *et al.*[8] reported the synthesis of sulfur-containing UV-curable acrylate oligomers. Akami *et al.*[13] studied the manufacturing method of 4,4'-thiodibenzenedithiol dimethacrylate. However, it exists in the solid state at room temperature and more importantly, it has a very limited solubility/compatibility with other UV resins. In our previous study, we synthesized new sulfur-containing aromatic difunctional acrylate monomers. These monomers have a high refractive indices, n_D^{20}=1.623-1.577 (liquid), and good optical transparencies.[14]

UV-curable formulations consist of acrylate oligomers and monomers which polymerize to form highly crosslinked polymer network as well as a photoinitiator which yields reactive initiating species upon UV exposure.[15-17] Generally, the final film properties may depend not only on the properties of the reactive components but also on the cure kinetics. If a sufficient conversion is not achieved, unreacted reactants

*Corresponding Author. E-mail: zahori@hanyang.ac.kr

yield material with less desirable properties and more aging stability. Therefore, the final conversion and UV-curing rates should be maximized. The oxygen concentration, temperature, light intensity, photoinitiator type and concentration are key factors that govern the polymerization kinetics and curing of the final coating. Therefore, to obtain the best physical and mechanical properties of the polymerization product, one must not only consider the materials used, but also the conditions under which the polymer was formed.[18-22] The kinetics of the photopolymerization reaction can be analyzed by photo-differential scanning calorimetry (photo-DSC). Photo-DSC offers a simple method to characterize the kinetics of photopolymerization reactions because it can be used to determine the kinetic parameters, reaction enthalpies, conversions and curing rates during the photopolymerization reaction.[19,23] Therefore, it has been used extensively to evaluate the kinetics of UV-curing systems and the technique is ideally suited for various conditions.[24-26] Several researchers have investigated the photopolymerization kinetics of acrylate. Anseth *et al.*[27] evaluated the kinetic constant for the photopolymerization of acrylate monomer. Young *et al.*[28] examined the effect of temperature on the isothermal curing kinetics. Cook *et al.*[29] studied the influence of temperature on the photopolymerization kinetics of a dimethacrylate series. Corcione *et al.*[30-32] studied the effect of the presence of oxygen on the free radical photopolymerization reaction, evaluated the kinetic reaction mechanism as functions of temperature and light intensity and attempted to correlate the experimental results with a theoretical and modeling approach.

In this paper, in order to optimize the coating physical properties, the polymerization kinetics of 3,3'-thiobis(1-(phenylthio)propane-3,2-diyl) diacrylate (SMDA) and 4,12-dioxo-6,10-bis(phenylthiomethyl)-3,13-dioxa-8-thia-5,11-diazapentadecane-1,15-diyl diacrylate (SMUA) were studied by utilizing photo-DSC. The kinetic characterization was carried out while varying the temperature, UV intensity, photoinitiator and the photoinitiator concentration. The activation energy was determined from an Arrhenius fit to the data.

Experimental

Materials. The materials used to synthesize 3,3'-thiobis(1-(phenylthio)propan-2-ol), thiophenol (>99%, Aldrich Co.), epichlorohydrin (ECH, >99%, Aldrich Co.) and sodium sulfide (>98%, Aldrich Co.) were used without further purification. Triethylamine (TEA, >99%, Aldrich Co.) was distilled before use. The materials used to synthesize 3,3'-thiobis(1-(phenylthio)propane-3,2-diyl) diacrylate, acrylic acid (AA, >99%, LG), toluene (>99%, Aldrich Co.), monomethyl ether hydroquinone (MEHQ, >99%, Eastman) and *p*-toluene sulfonic acid (>98%, Aldrich Co.) were used as purchased. The materials used to synthesize 4,12-dioxo-6,10-bis(phenylthiomethyl)-3,13-dioxa-8-thia-5,11-diazapentadecane-1,15-diyl diacrylate, dibutyltin dilaurate (DBTDL; >99%, Air Product) and 2-isocyanatoethyl acrylate (AOI, >99%, Showa denko) were used as purchased. *α*-Hydroxy-*α*-methylpropiophenone (Micure HP-8, Miwon), 2,2-dimethoxy-2-phenylacetophenone (Micure BK-6, Miwon), 2-phenylglyoxylic acid methyl ester (Micure MBF, Miwon), and 2-methyl-4'-(methylthio)-2-morpholinopropiophenone (Micure MS-7, Miwon) were utilized as photoinitiators. The overall reaction schemes to synthesize SMDA and SMUA are shown in Scheme I. All acrylate monomers were synthesized as previously described in the literature.[14]

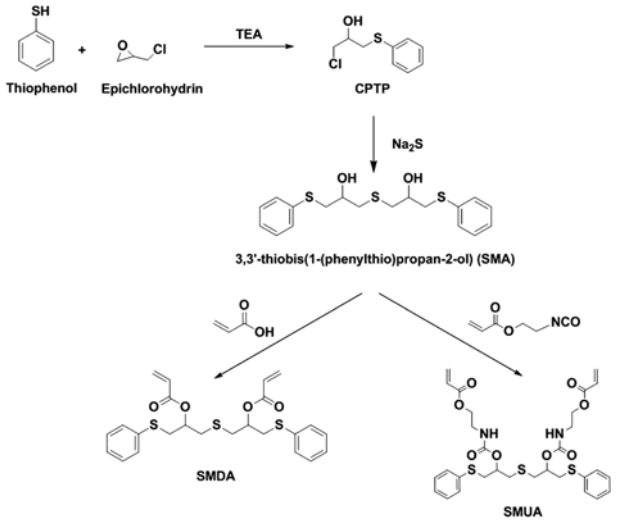

Scheme I. Overall reaction schemes for synthesis of SMDA and SMUA.

Synthesis.

Synthesis of 1-Chloro-3-(phenylthio)-2-propanol (CPTP): A mixture of thiophenol (150.00 g, 1.36 mol) and triethylamine (3.00 g, 0.03 mol) was placed in a 1 L, 4-necked flask equipped with a mechanical stirrer, N_2 inlet, thermocouple, and dropping funnel. The flask was cooled to 10 °C in an ice bath, and epichlorohydrin (126.70 g, 1.37 mol) was added dropwise. The solution was heated to 40 °C for 4 h. The reaction progress was determined by gas chromatography. Yield 99%; liquid; ^{1}H NMR ($CDCl_3$, 400 MHz) δ 7.36 (m, 2H), 7.28 (m, 2H), 7.20 (m, 1H), 3.90 (s, 1H), 3.65 (m, 2H), 3.20 (m, 2H), 2.96 (d, 1H).

Synthesis of 3,3'-Thiobis(1-(phenylthio)propan-2-ol) (SMA): 1-Chloro-3-(phenylthio)-2-propanol (184.00 g, 0.91 mol) was added to a 500 mL, 3-necked flask fitted with a mechanical stirrer, thermocouple, and dropping funnel at 40 °C, and 33% sodium sulfide (aq, 256.89 g, 0.5 mol) was added dropwise. The solution was then stirred for 10 h. The end of the reaction was determined by high performance liquid chromatography (HPLC). When the reaction was completed, toluene and deionized (D.I.) water were poured into the flask. The organic phase was washed with D.I. water, and the solvent was removed under vacuum at 50 °C. Yield 94%; white solid; ^{1}H NMR ($CDCl_3$, 400 MHz) δ 7.34 (m, 2H), 7.26 (m, 2H), 7.18 (m, 1H), 3.81 (m, 1H), 3.48 (d, 1H), 3.02 (m, 2H), 2.70 (m, 2H).

Synthesis of 3,3'-thiobis(1-(phenylthio)propane-3,2-diyl) Diacrylate (SMDA): A mixture of 3,3'-thiobis(1-(phenylthio) propan-2-ol) (79.40 g, 0.21 mol) in 100 mL of toluene, acrylic acid (37.46 g, 0.52 mol), 1.52 g of MEHQ, and 5.80 g of *p*-toluene sulfonic acid was placed in a 1-L, 4-necked flask equipped with a mechanical stirrer, N_2 inlet, thermocouple, and a Dean-Stark trap. The mixture was kept in the temperature range of 110-115 ºC and stirred for 10 h. The formed water was removed azeotropically. When the reaction was completed, the reaction was cooled to 60 ºC and a 10% NaOH solution was added. The organic phase was washed with D.I. water and the solvent was removed by evaporation *in vacuo*. The product was purified by vacuum distillation at 70 ºC followed by silica gel column chromatography (hexane:ethyl acetate = 85:15, v/v). Yield 90%; liquid; ^{1}H NMR ($CDCl_3$, 400 MHz) δ 7.32 (m, 2H), 7.20 (m, 2H), 7.10 (m, 1H), 6.28 (dd, 1H), 5.96 (dd, 1H), 5.79 (dd, 1H), 5.07 (m, 1H), 3.15 (m, 2H), 2.85 (m, 2H).

Synthesis of 4,12-dioxo-6,10-bis(phenylthiomethyl)-3,13-dioxa-8-thia-5,11-diazapentadecane-1,15-diyl Diacrylate (SMUA): 3,3'-Thiobis(1-(phenylthio)propan-2-ol) (50.22 g, 0.13 mol), 0.09 g of MEHQ, and 0.02 g of dibutyltin dilaurate were placed in a 500 mL, 4-necked flask under nitrogen equipped with a stirrer, thermocouple, and reflux condenser with a drying tube. 2-Isocyanatoethyl acrylate (38.67 g, 0.27 mol) was then added dropwise from the dropping funnel over 1h as the flask temperature was increased from 40 to 55 ºC. After holding for 1h, the contents were heated to 70 ºC and held for 5 h. The resulting monomer was analyzed by FTIR. The characteristic NCO band at 2269 cm^{-1} was no longer detectable. Yield 99%; liquid; ^{1}H NMR ($CDCl_3$, 400 MHz) δ 7.42 (m, 2H), 7.28 (m, 2H), 7.18 (m, 1H), 6.44 (dd, 1H), 6.15 (dd, 1H), 5.85 (dd, 1H), 5.57 (s, 1H), 5.01 (m, 1H), 4.20 (t, 2H), 3.42 (q, 2H), 3.20 (m, 2H), 2.85 (m, 2H).

Measurements. Photo-DSC measurements were carried out using a DSC instrument (Q-100, TA Instruments) equipped with a photocalorimetry accessory (Omnicure S2000). The light intensity was determined by placing an empty DSC pan on the sample cell. The UV light intensity at the sample was in the range of 5-30 mW/cm^2. The samples weighed approximately 10.0 mg. The measurements were carried out at 30 to 70 ºC under a nitrogen gas flow of 50 mL/min.

By integrating the area under the exothermic peak, the conversion of photopolymerization (C) was determined according to eq. (1):

$$C = \frac{\Delta H_{exp}}{\Delta H_{theo}} \quad (1)$$

where ΔH_{exp} is the experimental polymerization enthalpy, and ΔH_{theo} is the theoretical polymerization enthalpy (86.00 kJ/mol per acrylate double bond).[33]

Results and Discussion

Effect of the Photopolymerization Temperature. The effect of photopolymerization on the isothermal curing of a UV-curable monomer was studied with 5% Micure HP-8 as a photoinitiator (PI) at temperatures ranging from 30 to 70 ºC where the light intensity was held constant at 5 mW/cm^2. Figure 1 shows the photo-DSC heat flow curves for (a) SMDA and (b) SMUA obtained at different temperature. As the temperature increased, the peak maximum time tended to decrease in all of the samples. In SMDA, the maximum rate of photopolymerization in all of the samples was similar. In SMUA, the maximum rate of photopolymerization was achieved value at 60 ºC and then began to drop possibly due to depolymerization or decomposition.

Figure 2 shows the conversion versus time at different temperatures for (a) SMDA and (b) SMUA. In Figure 2(a), the final conversions were 15.6, 16.3, 16.5, 16.5, and 16.2% at temperatures of 30, 40, 50, 60, and 70 ºC, respectively. In Figure 2(b), the final conversions were 57.8, 63.5, 68.5, 71.9, and 71.4% at temperatures of 30, 40, 50, 60, and 70 ºC, respectively. The SMDA and SMUA conversions increased with increasing temperature up to 60 ºC. The slight decrease of the con-

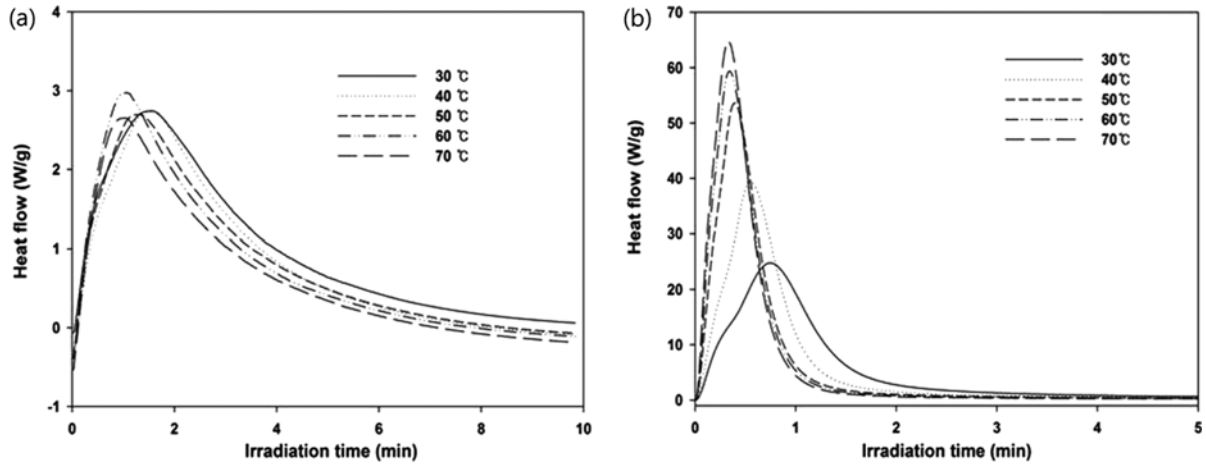

Figure 1. The photo-DSC heat flow thermograms recorded at different temperatures for (a) SMDA and (b) SMUA.

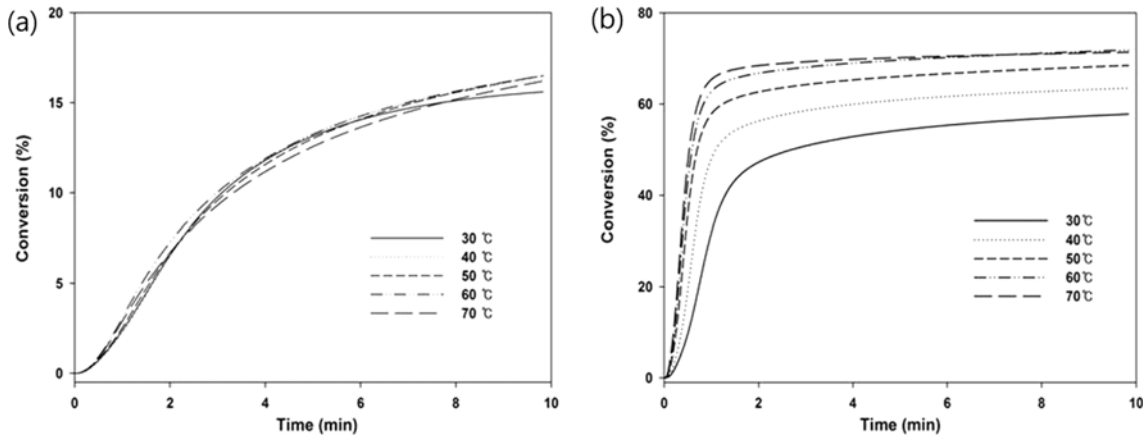

Figure 2. Plots of conversion versus time at different temperatures for (a) SMDA and (b) SMUA.

version at a temperature of 70 °C is due to depolymerization and competing reactions at high temperatures.

These phenomena can be confirmed by kinetic analysis. The photopolymerization of SMDA and SMUA creates poly SMDA and poly SMUA. We simplified the mathematical model of photopolymerization as follows

$PI \xrightarrow{h\nu} R\cdot$ Formation of initiating radicals

$R\cdot + M \rightarrow RM\cdot$ Initiation

$RM\cdot + nM \rightarrow RM_{n+1}\cdot$ Propagation

$R(M)_n\cdot + R(M)_m\cdot \rightarrow R(M)_n - (M)_mR$ Termination (coupling)

$R(M)_n\cdot + R(M)_m\cdot \rightarrow R(M)_n - H + R(M)_{m-1}M_{-H}$ Termination (disproportionation)

PI: Micure HP-8, M: SMDA or SMUA

Assuming that photopolymerization is first-order in the initial stage of the polymerization,[34,35] the rate constant of polymerization can be defined as shown in eq. (2).

$$-\frac{d[M]}{dt} = k[M] \quad (2)$$

or

$$X = 1\text{-}\exp(-kt) \quad (3)$$

Here, k refers to the first-order rate constant and X represents the conversion of SMDA and SMUA.

Figure 3 was created using eq. (3) and the slopes of the straight lines were used to calculate the first-order rate constant at each temperature. The calculated rate constants are listed in Table I and the corresponding Arrhenius plot is shown in Figure 4. As illustrated in Table I, the polymerization rate increased with increasing temperature up to 60 °C. From the Arrhenius plot, the activation energies of SMDA and SMUA are 3.95 and 36.01 kJ/mol, respectively. In Figure 4, the deviation of the correlation r from 1.0 with regards to Arrhenius fit was large due to change cure mechanism of the resin at different cure temperatures and due to depolymerization and competing reactions at high temperatures.[36-38]

Effect of Light Intensity. The light intensity was varied from 5-30 mW/cm^2 with a constant temperature of 60 °C and 5% Micure HP-8. Figure 5 shows the photo-DSC heat flow curves recorded at different light intensities for (a) SMDA and (b) SMUA. As the light intensity increased, the peak maximum

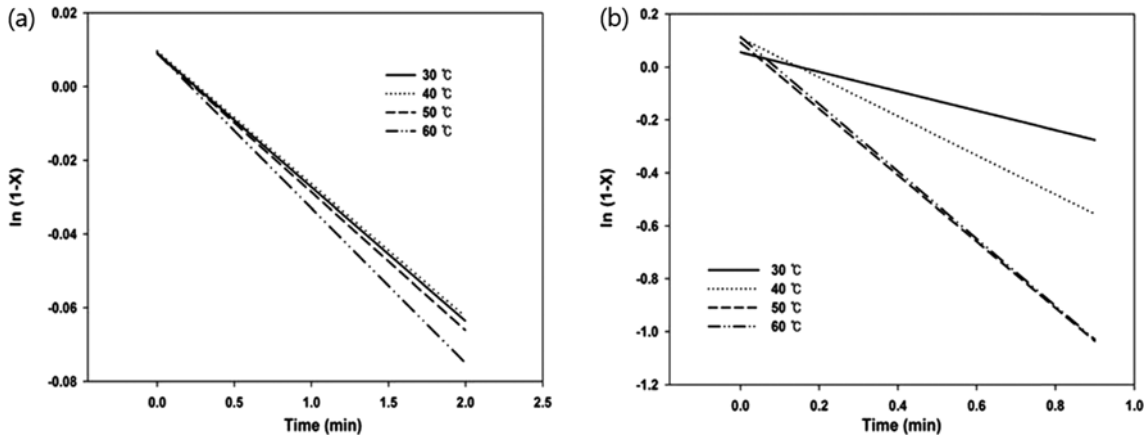

Figure 3. Plots of logarithm of unconverted fractions against the time at different reaction temperatures (a) SMDA and (b) SMUA.

Table I. First-Order Rate Constant and Activation Energies for the Photopolymerization of SMDA and SMUA at Different Temperatures

Temperature (°C)	Rate Constant (min^{-1}) for SMDA	E_a (kJ/mol) for SMDA	Rate Constant (min^{-1}) for SMUA	E_a (kJ/mol) for SMUA
30	0.0364	3.95	0.3675	36.01
40	0.0361		0.7384	
50	0.0376		1.2532	
60	0.0421		1.2697	

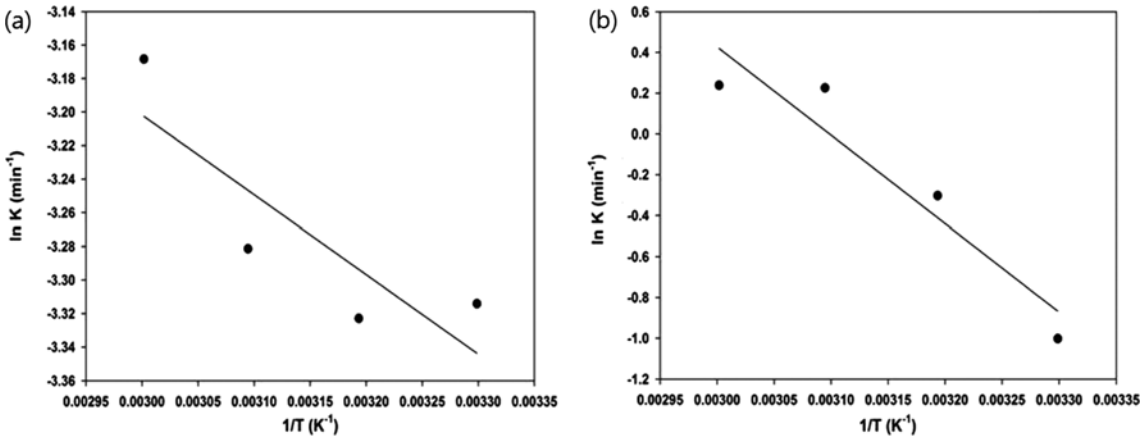

Figure 4. Arrhenius plots for photopolymerization of (a) SMDA and (b) SMUA.

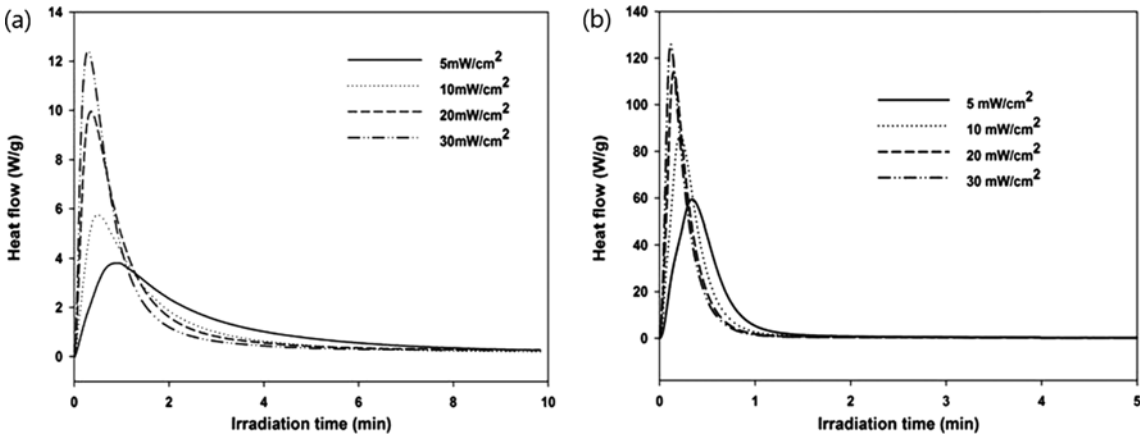

Figure 5. The photo-DSC heat flow thermograms recorded at different light intensities for (a) SMDA and (b) SMUA.

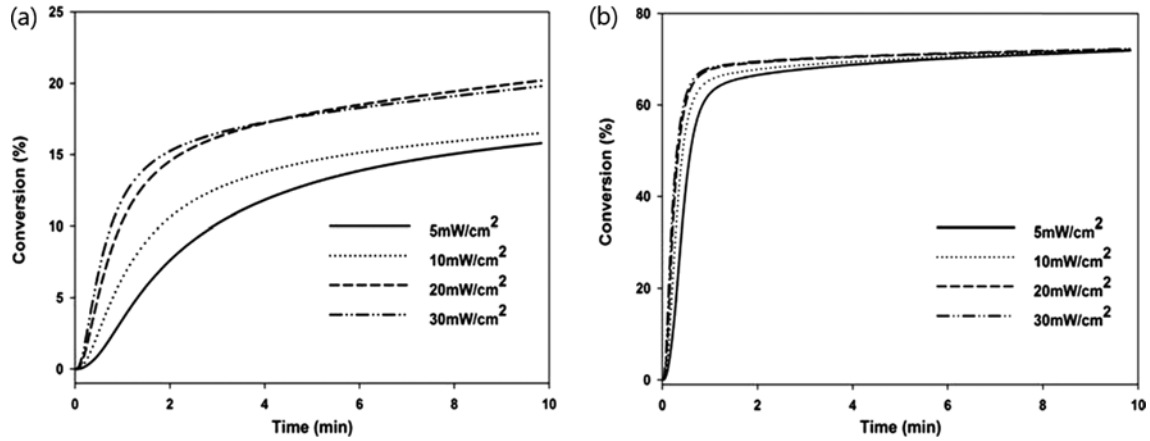

Figure 6. Plots of conversion versus time at different light intensities for (a) SMDA and (b) SMUA.

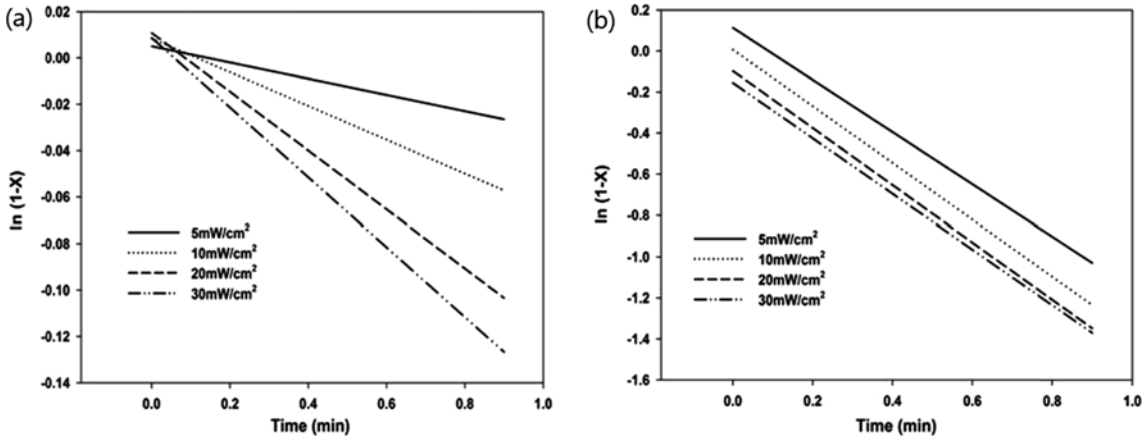

Figure 7. Plots of logarithm of unconverted fractions against the time at different light intensities for (a) SMDA and (b) SMUA.

time tended to decrease and the maximum rate of photopolymerization tended to increase in all of the samples. Figure 6 shows the conversions as a function of time obtaind for different light intensities for (a) SMDA and (b) SMUA. In Figure 6(a), the final conversions were 15.8, 16.5, 20.2, and 19.8% at light intensities of 5, 10, 20, and 30 mW/cm^2, respectively. In Figure 6(b), the final conversions were 71.9, 72.2, 72.1, and 72.3% at light intensities of 5, 10, 20, and 30 mW/cm^2, respectively. The SMDA conversion increased with increasing light intensity up to 20 mW/cm^2. At a light intensity of 30 mW/cm^2, the conversion decreased slightly. For SMUA, the conversions obtained at the various light intensities were similar. The slopes of straight lines were used to calculate the first-order rate constants at each light intensity, as shown in Figure 7. The calculated rate constants are listed in Table II. As the light intensity increased, the polymerization rate of SMDA increased. The polymerization rate of SMUA was the highest at a light intensity of 20 mW/cm^2.

Table II. First-Order Rate Constants for the Photopolymerization of SMDA and SMUA at Different Light Intensities

Light Intensity (mW/cm^2)	Rate Constant (min^{-1}) for SMDA	Rate Constant (min^{-1}) for SMUA
5	0.0421	1.2697
10	0.0729	1.3787
20	0.1269	1.3893
30	0.1503	1.3498

Effect of Concentration and Type of Photoinitiator (PI). The lowest light intensity that resulted in the optimal maximum conversion was 20 mW/cm^2 at a temperature of 60 °C. Therefore, the effect of the PI concentration was evaluated at 20 mW/cm^2 with HP-8 as the PI. The PI concentration was varied from 1-10%. Figure 8 shows the photo-DSC heat flow thermograms recorded with different PI concentrations for (a) SMDA and (b) SMUA. As the PI concentration for SMDA increased, the peak maximum time tended to decrease because the number of propagating chains in the system increased and the maximum rate of photopolymerization tended to increase because diffusion-controlled termination had more influence than diffusion-controlled propagation. As the PI concentration of SMUA increased, the peak maximum time decreased and the maximum rate of photopolymerization increased up to 5% PI and then decreased slightly. Figure 9 shows the conversion as a function of time with different PI concentrations for (a) SMDA and (b)

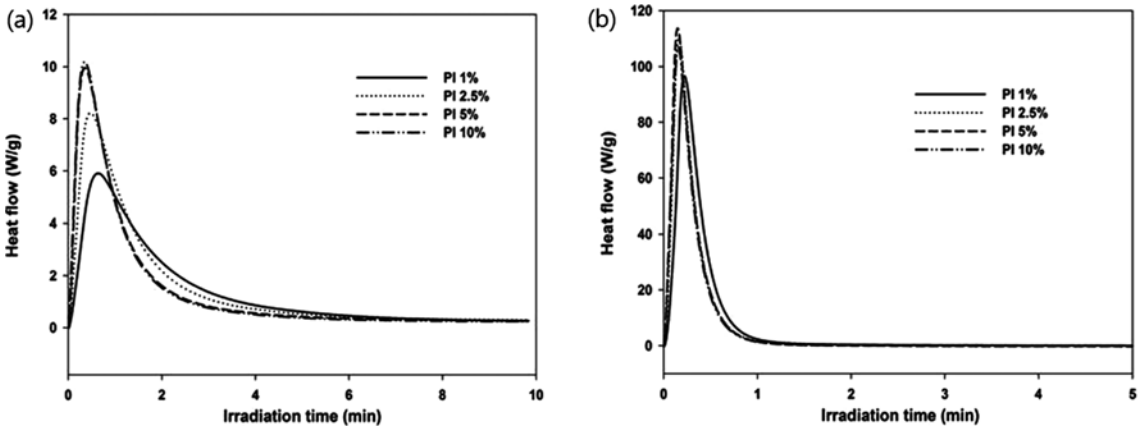

Figure 8. The photo-DSC heat flow thermograms recorded at different concentrations of PI for (a) SMDA and (b) SMUA.

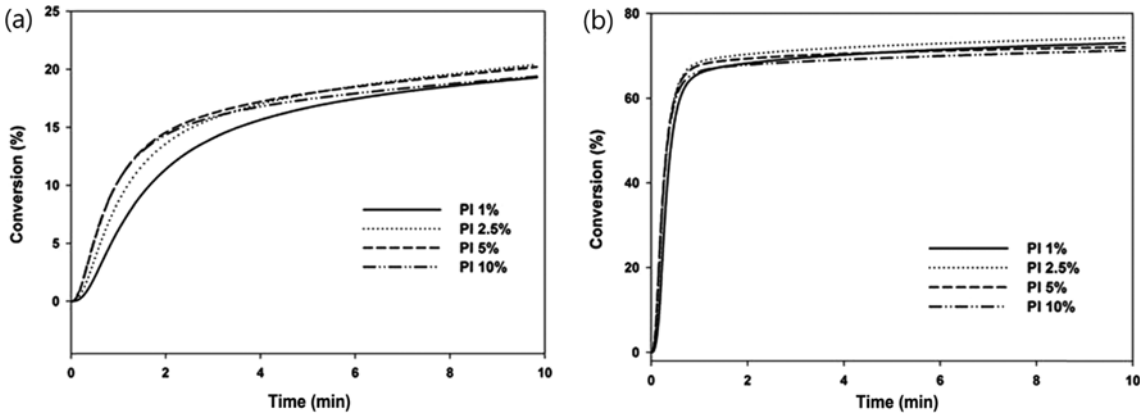

Figure 9. Plots of conversion versus time with different concentrations of PI for (a) SMDA and (b) SMUA.

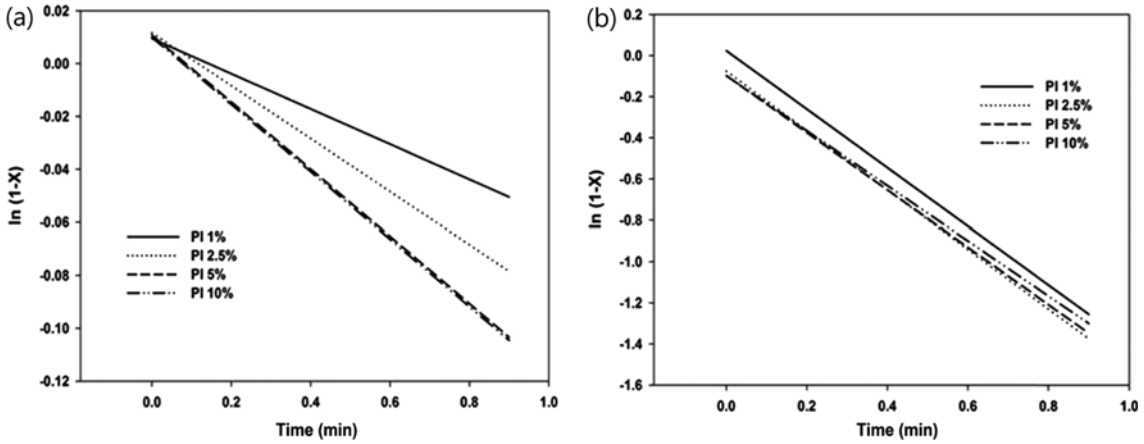

Figure 10. Plots of logarithm of unconverted fractions against the time at different concentrations of PI for (a) SMDA and (b) SMUA.

Table III. First-Order Rate Constant for the Photopolymerization of SMDA and SMUA Obtained at Different PI Concentrations

Photoinitiator Concentration (%)	Rate Constant (min^{-1}) for SMDA	Rate Constant (min^{-1}) for SMUA
1	0.0666	1.4208
2.5	0.1001	1.4418
5	0.1269	1.3893
10	0.1272	1.3352

SMUA. For SMDA, the final conversions were 19.3, 20.4, 20.2 and 19.4% at PI concentrations of 1, 2.5, 5, and 10%, respectively. For SMUA, the final conversions were 73.0, 74.3, 72.1, and 71.3% at PI concentrations of 1, 2.5, 5, and 10%, respectively. The maximum conversion of each monomer occurred at a PI concentration of 2.5% because of the high rate of recombination. The slopes of the straight lines were used to calculate the first-order rate constants with different PI concentrations and are shown in Figure 10. The calculated rate constants are listed in Table III. As the PI concentration increased, the polymerization rate constant of SMDA increased, but that of SMUA was the highest at a PI concentration of 2.5%.

Various PIs were cured at 2.5% PI, 60 °C, and a light intensity of 20 mW/cm^2. Figure 11 shows the photo-DSC heat flow curves recorded with various PIs for (a) SMDA and (b) SMUA. SMDA had a maximum rate of photopolymerization and a peak maximum time with MBF followed by MS-7, HP-8,

Table IV. Photopolymerization Rate Constants and Conversions of Photopolymerization of SMDA and SMUA Obtained with Different PIs

Photoinitiator	Rate Constant (min^{-1}) for SMDA	Conversion (%) for SMDA	Rate Constant (min^{-1}) for SMUA	Conversion (%) for SMUA
HP-8	0.1001	20.4	1.4418	74.3
BK-6	0.1498	20.8	1.4187	72.2
MS-7	0.1019	18.8	1.2104	67.7
MBF	0.0148	13.5	0.8743	67.0

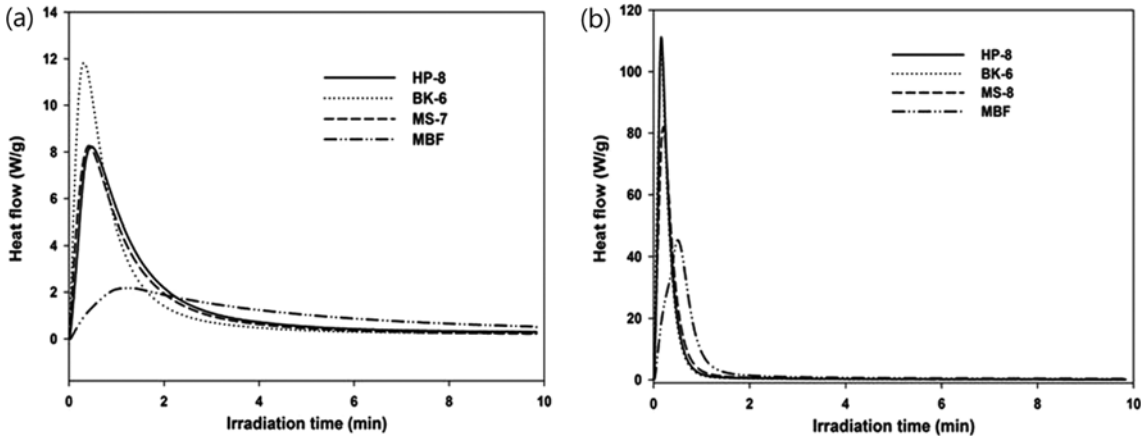

Figure 11. The photo-DSC heat flow thermograms recorded with different types of PI for (a) SMDA and (b) SMUA.

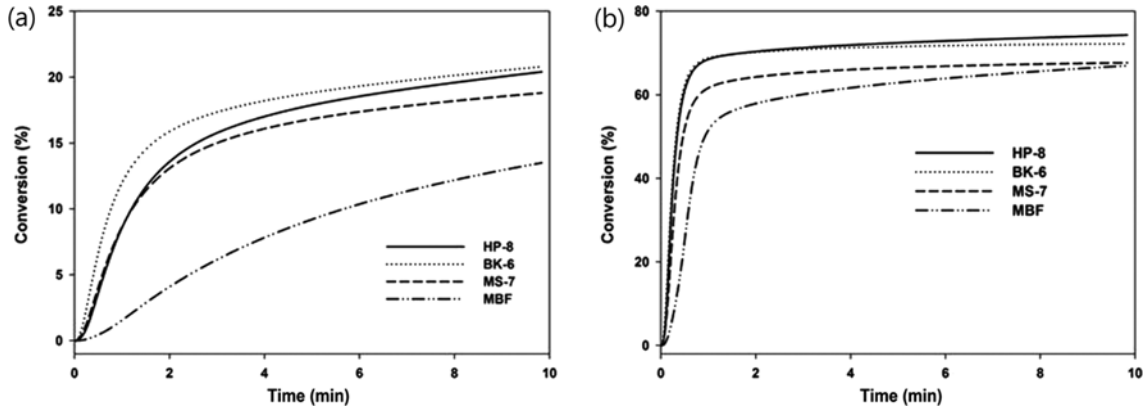

Figure 12. Plots of conversion versus time with different types of PI for (a) SMDA and (b) SMUA.

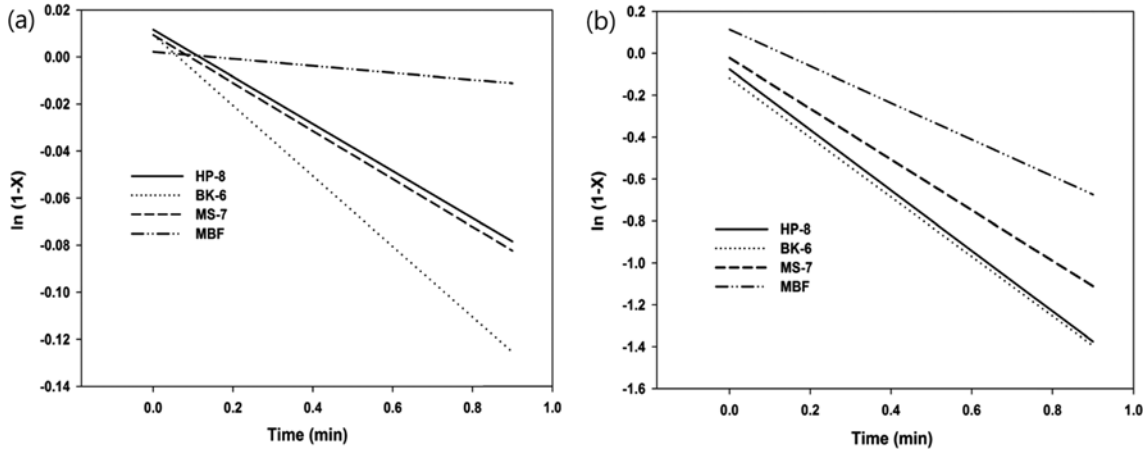

Figure 13. Plots of logarithm of unconverted fractions against the time with different types of PI for (a) SMDA and (b) SMUA.

and BK-6. SMUA had a maximum rate of photopolymerization and peak maximum time with MBF followed by MS-7, BK-6, and HP-8. Figure 12 shows the conversion as a function of time with different PIs for (a) SMDA and (b) SMUA. The SMDA conversions with HP-8, BK-6, MS-7, and MBF were 20.4, 20.8, 18.8, and 13.5%, respectively. The SMUA conversions with HP-8, BK-6, MS-7, and MBF were 74.3, 72.2, 67.7, and 67.0%, respectively. The slopes of the straight lines were used to calculate the first-order rate constants for each PI and are shown in Figure 13. The calculated rate constants are listed in Table IV. The SMDA polymerization rate constants were the lowest for MBF followed by HP-8, MS-7, and BK-6.

The SMUA polymerization rate constants were the lowest for MBF followed by MS-7, BK-6, and HP-8. Using BK-6 as a photoinitiator created the highest conversion of polymerization for acrylate and HP-8 for urethane acrylate.

Conclusions

The photopolymerization kinetics of 3,3'-thiobis(1-(phenylthio)propane-3,2-diyl) diacrylate (SMDA) and 4,12-dioxo-6,10-bis(phenylthiomethyl)-3,13-dioxa-8-thia-5,11-diazapentadecane-1,15-diyl diacrylate (SMUA) were investigated by photo-differential scanning calorimetry. The effects of various parameters such as the UV intensity, temperature, photoinitiator concentration, and initiator type were evaluated. In SMDA, as the temperature and light intensity increased, the peak maximum time tended to decrease. The conversion increased with increasing temperature up to 60 °C and increasing light intensity up to 20 mW/cm^2. However, at 70 °C and 30 mW/cm^2, the conversion decreased slightly due to depolymerization and competing reactions. As the PI concentration increased, the peak maximum time decreased and polymerization rate constant increased. With a PI concentration of 2.5%, the highest conversion of polymerization could be achieved, with BK-6 resulting in the highest conversion among the PIs. In SMUA, the maximum photopolymerization rate reached the maximum value at 60 °C and after which it began to decrease, possibly due to depolymerization or decomposition. The polymerization rate was the highest at a light intensity of 20 mW/cm^2. The highest maximum conversion and polymerization rate constant were achieved at a PI concentration of 2.5%. Also, the highest conversion of polymerization was achieved with HP-8. The activation energies of SMDA and SMUA were 3.95 and 36.01 kJ/mol, respectively.

Acknowledgment. This work was supported by the research fund of Hanyang University (HY-2012-P).

References

(1) J. F. Rabek, *Mechanisms of Photophysical abd Photochemcial Reactions in Polymers, Theory and Practical Applications,* Wiley, New York, 1987.
(2) H. Hwang, C. Park, J. Moon, H. Kim, and T. Masubuchi, *Prog. Org. Coat.*, **72**, 663 (2011).
(3) A. Fieberg and O. Reis, *Prog. Org. Coat*., **45**, 239 (2002).
(4) C. Decker, *Macromol. Rapid Commun*., **23**, 1067 (2002).
(5) C. Lowe and P. K. T. Oldring, *Chemistry and Technology of UV and EB Formulations for Coatings, Inks and Paints,* Vol. IV, SITA Press, London, 1991.
(6) B. Karagoz and N. Bicak, *Eur. Polym J*., **44**, 106 (2008).
(7) A. Nakamura, H. Fujii, N. Juni, and N. Tsutsumi, *Opt. Rev.*, **1**, 104 (2008).
(8) A. Nebioglu, J. A. Leon, and I. V. Khudyakov, *Ind. Eng. Chem. Res*., **47**, 2155 (2008).
(9) J. G. Liu and M. Ueda, *J. Mater Chem*., **19**, 8907 (2009).
(10) S. Ando, T. Fujigaya, and M. Ueda, *Jpn. J. Appl. Phys*., **41**, L105 (2002).
(11) T. Matsuda, Y. Funae, M. Yoshida, T. Yamamoto, and T. Takaya, *J. Appl. Polym. Sci*., **76**, 50 (2000).
(12) R. Okutsu, Y. Suzuki, S. Ando, and M. Ueda, *Macromolecules*, **41**, 6165 (2008).
(13) A. Hidehiko and Y. Katsumasa, JP Patent 2013155118 (2013).
(14) J. S. Kim, B. S. Cho, J. O. Kweon, and S. T. Noh, *Prog. Org. Coat*., **77**, 1695 (2014).
(15) M. Suwa, H. Niwa, and M. J. Tomikawa, *Photopolym. Sci. Technol*., **19**, 275 (2006).
(16) J. Nakai and T. Aoki, US Patent 7087945 (2006).
(17) K. Mori and T. Tano, JP Patent 2007056048 (2007).
(18) C. Decker, *Acta Polym*., **45**, 333 (1994).
(19) J. G. Kloosterboer, *Adv. Polym. Sci*., **84**, 1 (1998).
(20) C. E. Corcione, A, Greco, and A. Maffezoli, *Polymer*, **46**, 8018 (2005).
(21) D. Avci, J. Nobles, and L. J. Mathias, *Polymer*, **44**, 963 (2003).
(22) T. F. Scottt, W. D. Cook, and J. S. Forsythe, *Polymer*, **44**, 671 (2003).
(23) T. Doornkamp and Y. Y. Tan, *Polym. Commun*., **31**, 362 (1990).
(24) T. Scherzer and U. Decker, *Vib. Spectrosc*., **19**, 385 (1999).
(25) D. P. Dworak and M. D. Soucek, *Prog. Org. Coat*., **47**, 448 (2003).
(26) T. F. Scottt, W. D. Cook, and J. S. Forsythe, *Polymer*, **43**, 5839 (2002).
(27) K. S. Anseth, C. M. Wang, and C. N. Bowman, *Polymer*, **35**, 3243 (1994).
(28) J. S. Young and C. N. Bowman, *Macromolecules,* **32**, 6073 (1999).
(29) W. D. Cook, *J. Polym. Sci. Part A: Polym. Chem*., **31**, 1053 (1993).
(30) C. E. Corcione and M. Frigione, *Thermochim. Acta*, **534**, 21 (2012).
(31) C. E. Corcione, A. Previderio, and M. Frigione, *Thermochim. Acta*, **509**, 56 (2010).
(32) C. E. Corcione, A. Grrco, and A. Maffezzoli, *J. Appl. Polym. Sci*., **92**, 3484 (2004).
(33) E. Andrejewska and M. Andrzejewski, *J. Polym. Sci. Part A: Polym. Chem*., **36**, 665 (1998).
(34) A. Maffezzoli and R. Terzi, *Thermochim. Acta*., **321**, 111 (1998).
(35) E. W. Nelson, T. P. Carter, and A. B. Scranton, *Polymer*, **36**, 4651 (1995).
(36) P. Castell, M. Wouters, H. Fischer, and G. de with, *J. Coat. Technol. Res.,* **4**, 411 (2007).
(37) E. Andrzejewska, *Polymer*, **37**, 1047 (1996).
(38) D. J. Broer, G. N. Mol, and G. Challa, *Polymer,* **32**, 690 (1991).